International Journal of High-Rise Buildings
December 2012, Vol 1, No 4, 247-254

International Journal of
High-Rise Buildings
www.ctbuh.org

Simplified Algorithm of the Novel Steel-concrete Mixed Structure under Lateral Load

Liang Li[1], Guo-qiang Li[2†], and Yu-shu Liu[3]

[1]*College of Civil Engineering, Chang'an University, Xi'an 710061, China*
[2]*State Key Laboratory for Disaster Reduction in Civil Engineering, Tongji University, Shanghai 200092, China*
[3]*College of Civil Engineering, Tongji University, Shanghai 200092, China*

Abstract

In order to improve the seismic behaviors of traditional steel-concrete mixed structure, a novel steel concrete mixed structure consisting of steel frames braced with buckling restrained braces (BRBs) and a concrete tube is proposed. Based on several assumptions, the simplified mechanical model of the novel mixed structure is established, and the shear and bending stiffness formulas of the steel frames, BRBs and concrete tube are respectively introduced. The equilibrium differential equation of the novel mixed structure under horizontal load is developed based on the structural elastic theory. The simplified algorithms to determine the lateral displacement and internal forces of the novel mixed structure under the inverted-triangle distributed load, uniformly load and top-concentrated load are then obtained considering several boundary conditions and compatible deformation conditions. The effectiveness of the simplified algorithms is verified by FEM comparison.

Keywords: Steel-concrete mixed structure, Buckling restrained braces, Hinged frame with BRB, Equilibrium differential equations, Elastic theory, Simplified algorithm

1. Introduction

Traditional steel-concrete mixed structure is composed of steel frame and concrete core tube, which may take advantages of steel structure and concrete structure since the vertical resistant efficiency of the steel frame is high, while the lateral resistant efficiency of the concrete core-tube is high (Gregory and Hiroshi, 2004; Lu, Qin, and Luo, 2009; Li, Shi, and Wang, 2009). However, there are still some deficiencies existed in such steel-concrete mixed structure. First of all, the ductility of the welding or welding-bolt connection for traditional steel frames is poor, and the brittle failures are liable to happen during earthquakes (Anli, 2005; Eurocode 4, 2004; Hu, 2008). Secondly, excessive section sizes of the steel frame components are required to resist the internal force increased with damage of the concrete tube during the earthquakes. However it is very ineffective to improve the lateral resistant capacity of the steel frame by enlarging the section of the frame beams and columns.

Considering that: (1) the ductility of semi-rigid connection is excellent, which can remain a stable flexural capacity in great plastic deformation, so the brittle failure may be avoided with semi-rigid beam-column connection (Duane, 1998; Wang and Zhou, 2011); (2) the moment distribution of the steel-concrete composite beam can be optimized by adjusting the rotational stiffness of the beam-to-column connection, so the consumption of steel can be reduced (Li, Shi, and Wang, 2009; Yao, Bai, and Dang, 2010); (3) the buckling restraint brace (BRB) can reach yielding at tension or compression, and provide great lateral stiffness and load-bearing capacity to the steel structure with excellent energy dissipation capability (Koz, 2002; Li, Shi, and Wang, 2009), a new steel-concrete mixed structure is proposed. This new mixed structure consists of steel frames with semi-rigid connections, BRBs and concrete tube, as shown in Fig. 1 below.

The arrangement of BRBs should follow the principles below:

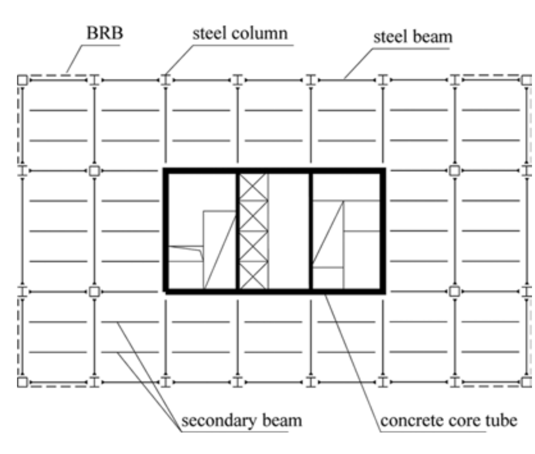

Figure 1. Plan view of the multi-lateral resistant steel-concrete mixed structure.

†Corresponding author: Guo-Qiang Li
Tel: +86-21-6598-2975; Fax: +86-21-6598-3431
E-mail: gqli@tongji.edu.cn

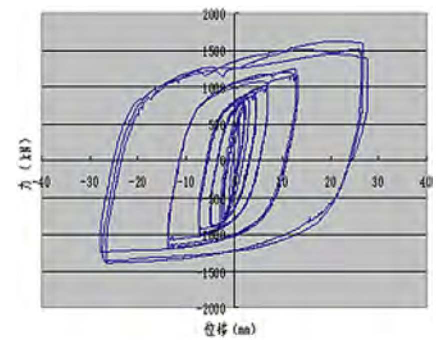

Figure 2. Tested N-δ relationship of BRBs.

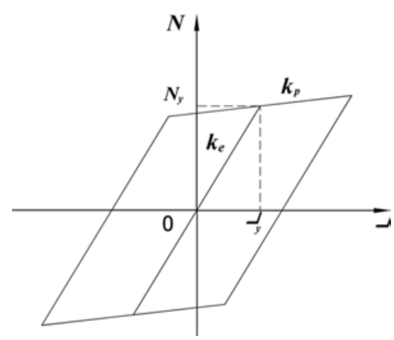

Figure 3. Bilinear N-δ model of BRBs.

(1) The vertical distribution of BRBs should be continuous along the height of the building, and should be extended to the foundations of the building with basement;

(2) The arrangement of BRBs should be symmetrical in the plane of the building.

Test results show that the tensile and compressive properties of the BRBs are similar under the action of repeated axial forces, and the hysteretic loop of N-δ is very full (Li, 2011), as shown in Fig. 2. The axial force-deformation relation of BRBs agrees quite well with the bilinear model, and BRBs can be simulated with bilinear model link element to consider the yielding phenomenon and energy dissipation of BRBs, as shown in Fig. 3.

Some theoretical studies on the design methods and seismic behavior of this new steel-concrete mixed structure have been conducted (Li, Shi, and Wang, 2009; Li, 2011). Several stiffness ratios are proposed to show the relative stiffness between steel frame, BRBs and concrete tube. The relationship between the story drift and the stiffness ratio of the novel mixed structure is studied, and the optimal stiffness ratio is suggested. The simplified calculation method for elasto-plastic lateral displacement of this novel mixed structure in severe earthquakes is proposed based on the effective damping ratio method of the equivalent linearization method.

2. Simplified Mechanical Model and Assumption

According to the equivalent stiffness principles, the steel frames, BRBs and concrete core tube can be equivalent to the planar overall frame, planar hinged frame with BRBs and planar overall shear walls respectively, and they can be further simplified as the parallel cantilevers mode, as shown in Fig. 4.

For simplifying formulation, the following assumptions are employed(Bao, 2001; Wang and Zhou, 2010; Li, Shi, and Wang, 2009):

(1) the sections of the frame, BRBs and concrete core tube keep constant along the height of the building;

(2) the planar overall frame, planar hinged frame with BRBs and planar overall shear wall are linked to each other by infinitely rigid bars which are continuously distributed along the height of the building. Equation Section 3.

3. Stiffness Calculations

3.1. Steel frame with semi-rigid connection

The lateral stiffness of the column i at story j of the

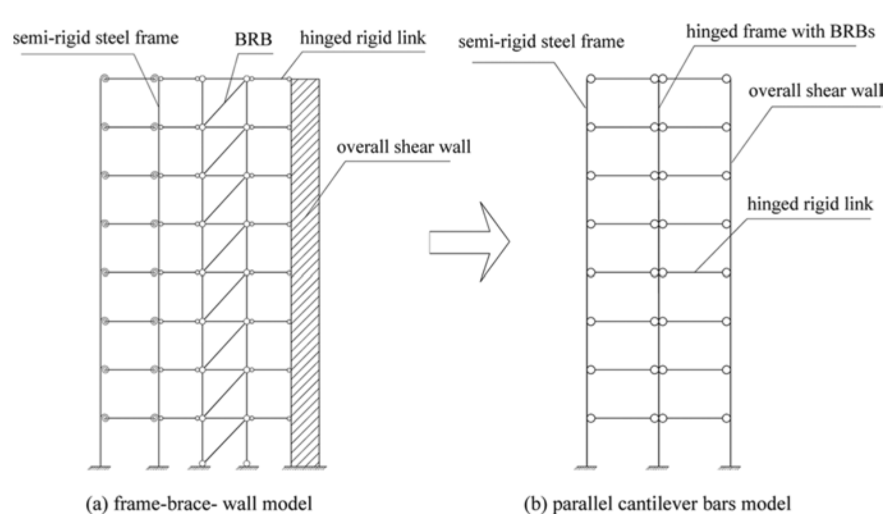

Figure 4. Simplified mechanical model of the novel multi lateral-resistant mixed structure.

Table 1. Correction factor of the column $\beta_{i,j}$

Floor		Schematic diagram	$\beta_{i,j}$
Middle floor		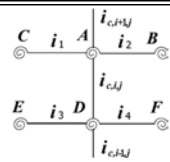	$\beta_{i,j}=\dfrac{6i_{c,i,j}+6i_{c,i+1,j}}{6i_{c,i,j}+6i_{c,i+1,j}+k_{AC,3}+k_{AA,3}+k_{AA,4}+k_{AB,4}}$
Base floor	Fixed end	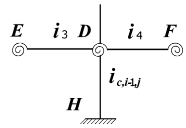	$\beta_{i,j}=\dfrac{6i_{c,i,j}+4i_{c,i-1,j}}{6i_{c,i,j}+4i_{c,i-1,j}+k_{DF,1}+k_{DD,1}+k_{DD,2}+k_{DE,2}}$
	Hinged end	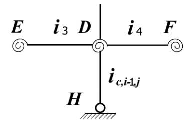	$\beta_{i,j}=1-\dfrac{6i_{c,i,j}+3i_{c,i-1,j}}{6i_{c,i,j}+3i_{c,i-1,j}+k_{DF,1}+k_{DD,1}+k_{DD,2}+k_{DE,2}}$
Top floor		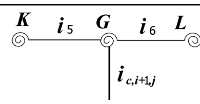	$\beta_{i,j}=1-\dfrac{6i_{c,i+1,j}}{6i_{c,i+1,j}+k_{GK,5}+k_{GG,5}+k_{GG,6}+k_{GL,6}}$

steel frame with semi-rigid connections can be expressed as (Hu, 2008)

$$D_{i,j}=\beta_{i,j}\sum_{j=1}^{n}\frac{12i_{c,i,j}}{h_i^2} \tag{1}$$

where

$\beta_{i,j}$: correction factor of the column j at story i while considering the influence of semi-rigid connections (Shi-hua, 2001), see Table 1;

$i_{c,i,j}$: linear stiffness of column j at story i;

h_i : height of the story i.

The shear stiffness of the frame at story i can be expressed as

$$C_{f,i}=h_i\sum D_{i,j} \tag{2}$$

The flexural stiffness of the frame at storey i can be expressed as (Chinese code, 1998)

$$(E_fI_f)_i=E_f\sum_{j=1}^{n}(I_{ij}+A_{ij}c_{ij}) \tag{3}$$

where

E_f : steel elastic modulus of the column;

I_{ij} : section inertia of the column j at story i;

A_{ij} : section area of the column j at story i;

c_{ij} : distance from the column j at story i to the neutral axis.

3.2. Hinged frame with BRB

The shear stiffness offered by BRBs at story i can be expressed as (Li, Shi, and Wang, 2009; Hu, 2008)

$$C_{b,i}=h_i\sum_{j=1}^{n}D_{b,ij}=h_i\sum_{j=1}^{n}k_{ij}cos^2\theta_{ij} \tag{4}$$

where

k_{ij} : axial stiffness of the BRB j at story i;

θ_{ij} : angle from the axial direction of the BRB j at story i to horizontal direction.

While considering the effect of axial deformation of steel columns, the bending rigidity of hinged frame with BRBs can be expressed as (Chinese code, 1998)

$$(E_bI_b)_i=E_{bc}\mu'\sum_{i=1}^{n}(I_{ij}+A_{ij}c_{ij}) \tag{5}$$

where

μ' : reduction coefficient, desirable value should be 0.8~0.9 for the center brace;

E_{bc} : elastic modulus of the column in hinged frame with BRB;

A_{ij} : section area of the column j at story i.

The shear deformation effect coefficient γ_b^2 of the hinged frame with BRBs can be expressed as

$$\gamma_b^2=\frac{E_bI_b}{C_{b,i}H^2} \tag{6}$$

where

H : total height of the concrete core tube.

According to the principle of equal top displacement, the equivalent bending stiffnessof the hinged frame with BRBs can be expressed as

$$\left.\begin{aligned}(E_bI_b)_{eq}&=\frac{E_bI_b}{1+3.64\gamma_b^2}\quad\text{(Inverted triangle load)}\\(E_bI_b)_{eq}&=\frac{E_bI_b}{1+4\gamma_b^2}\quad\text{(Uniformly distributed load)}\\(E_bI_b)_{eq}&=\frac{E_bI_b}{1+3\gamma_b^2}\quad\text{(Top concentrated load)}\end{aligned}\right\} \tag{7}$$

3.3. Concrete core tube

The shear deformation effect coefficient γ_t^2 of the concrete core tube can be given as

$$\gamma_t^2=\frac{\mu E_t I_t}{G_t A_t H^2} \tag{8}$$

where

E_t : elastic modulus of the concrete;
I_t : section inertia of the concrete core tube;
μ : shear stress non-uniform coefficient;
G_t : shear elastic modulus of concrete;
A_t : cross-sectional area of the concrete core tube.

According to the equal top displacement principle, the equivalent stiffness of the concrete core tube can be expressed as (Bao, 2001)

$$\left.\begin{aligned}
&(E_tI_t)_{eq}=\frac{E_bI_b}{1+3.64\gamma_b^2} &&\text{(Inverted triangle load)}\\
&(E_tI_t)_{eq}=\frac{E_bI_b}{1+4\gamma_b^2} &&\text{(Uniformly distributed load)}\\
&(E_tI_t)_{eq}=\frac{E_bI_b}{1+3\gamma_b^2} &&\text{(Top concentrated load)}
\end{aligned}\right\} \tag{9}$$

4. Establishment of the Differential Equation

Under arbitrary distribution lateral load $q(z)$, simplified mechanical model of the novel steel-concrete mixed structure is shown in Fig. 5(a).

The moment at height z equals to the summation of the three components

$$M(z)=M_f(z)+M_b(z)+M_t(z) \tag{10}$$

where

$M_f(z)$: moment loaded on the steel frame with semi-rigid connection;
$M_b(z)$: moment loaded on BRBs
$M_t(z)$: moment loaded on the concrete tube.

According to the moment equilibrium equation $\Sigma M=0$ in Fig. 5(b), the following equation can be arrived

$$Q(z)=Q_t(z)+Q_b(z)+Q_f(z)=\frac{dM(z)}{dz} \tag{11}$$

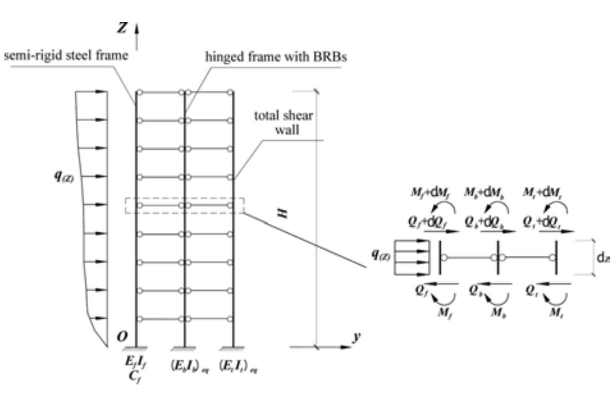

Figure 5. Simplified model and internal force.

Again based on the shear equation $\Sigma Q=0$, it can get

$$q(z)=q_t(z)+q_b(z)+q_f(z)=-\frac{dQ(z)}{dz} \tag{12}$$

According to the compatible deformation conditions, it can be given as

$$\frac{d^2y}{dz^2}=\frac{d^2y_t}{dz^2}=\frac{d^2y_b}{dz^2}=\frac{d^2y_f}{dz^2}=\frac{d^2y_{f,M}}{dz^2}+\frac{d^2y_{f,Q}}{dz^2} \tag{13}$$

where

$y_t(z)$: lateral displacement of the concrete core tube;
$y_b(z)$: lateral displacement of the hinged frame with BRBs;
$y_f(z)$: lateral displacement of the semi-rigid steel frame;
$y_{f,M}(z)$: bending portion of the lateral displacement of the semi-rigid frame;
$y_{f,Q}(z)$: shear portion of the lateral displacement of the semi-rigid frame.

From the relationship between internal forces and deformations, we have

$$\left.\begin{aligned}
&M_t(z)=-(E_tI_t)_{eq}\frac{d^2y}{dz^2}\\
&M_b(z)=-(E_bI_b)_{eq}\frac{d^2y}{dz^2}\\
&M_f(z)=-E_fI_f\frac{d^2y_{f,M}}{dz^2}
\end{aligned}\right\} \tag{14}$$

Substituting Eqs. (13) and (14) into Eq. (10), it can be arrived that

$$[(E_bI_b)_{eq}+(E_bI_b)_{eq}+E_fI_f]\frac{d^2y}{dz^2}=-M(z)+E_fI_f\frac{d^2y_{f,Q}}{dz^2} \tag{15}$$

Based on material mechanics, we may know that:

$$\frac{dy_{f,Q}}{dz}=\frac{Q_f(z)}{C_f} \tag{16}$$

After the second derivation of Eq. (16), and taking the result into Eq. (12), the following expression can be arrived

$$\frac{d^2y_{f,Q}}{dz^2}=\frac{1}{C_f}\frac{dQ_f(z)}{dz}=\frac{q(z)-q_t(z)-q_b(z)}{C_f} \tag{17}$$

Substituting Eq. (11) and Eq. (14) into Eq. (15), we know that

$$\left.\begin{aligned}
&q_t(z)=(E_tI_t)_{eq}\frac{d^4y}{dz^4}\\
&q_b(z)=(E_bI_b)_{eq}\frac{d^4y}{dz^4}\\
&q_f(z)=E_fI_f\frac{d^4y_{f,M}}{dz^4}
\end{aligned}\right\} \tag{18}$$

Then substituting Eqs. (17) and (18) into Eq. (15), and letting $\xi = z/H$, $\Sigma EI = E_f I_f + (E_t I_t)_{eq} + (E_b I_b)_{eq}$, then we can get

$$\frac{d^4y}{d\xi^4}-\lambda^2\frac{d^2y}{d\xi^2}=\frac{M(z)}{\Sigma EI}\lambda^2H^2+\frac{q(z)H^4}{(E_tI_t)_{eq}+(E_bI_b)_{eq}} \tag{19}$$

where $\lambda = H\sqrt{C_f\Sigma EI/E_fI_f[(E_tI_t)_{eq}+(E_bI_b)_{eq}]}$, which is a parameter related with the bending and shear stiffness of the steel frame, BRBs and concrete core tube.

5. Simplified Algorithm of Lateral Displacement

5.1. Under inverted triangle lateral load

Under inverted triangle lateral load, the load density and bending moment at height ξ can be expressed as

$$q(\xi)=q(H)\xi \tag{20}$$

$$M(\xi)=-\frac{q(H)H^2}{6}(2-3\xi+\xi^3) \tag{21}$$

Substituting Eqs. (20) and (21) into Eq. (19), we may obtain the following fourth-order differential equation as

$$\frac{d^4y}{d\xi^4}-\lambda^2\frac{d^2y}{d\xi^2}=-\frac{q(H)H^4}{6\Sigma EI}\lambda^2\xi^3+\left[\frac{q(H)H^4}{2\Sigma EI}\lambda^2+\frac{q(H)H^4}{(E_tI_t)_{eq}+(E_bI_b)_{eq}}\right]\xi-\frac{q(H)H^4}{3\Sigma EI}\lambda^2 \tag{22}$$

The general solution of Eq. (22) is

$$y=A_1+A_2\xi+A_3\mathrm{sh}\lambda\xi+A_4\mathrm{sh}\lambda\xi+y^* \tag{23}$$

In Eq. (23), the special solution can be expressed as

$$y^*=B_1\xi^5+B_2\xi^5+B_3\xi^5 \tag{24}$$

In Eqs. (23) and (24), there are seven unknown coefficients named A_1~A_4, and B_1~B_3.

Substituting Eq. (24) into Eq. (22)we can get

$$y^*=\frac{q(H)H^4}{120\Sigma EI}\xi^5+\frac{q(H)H^4}{6\lambda^2}\left(\frac{1}{\Sigma EI}-\frac{1}{(E_tI_t)_{eq}+(E_bI_b)_{eq}}\right)-\frac{q(H)H^4}{12\Sigma EI}\xi^3+\frac{q(H)H^4}{6\Sigma EI}\xi^2 \tag{25}$$

The seven constants of the general solution can be determined by geometric and natural boundary conditions $y|_{\xi=0}=0$, $y'|_{\xi=0}=0$, $y''|_{\xi=1}=0$. We can get

$$\left.\begin{aligned}
&A_1=-A_4=A_3\frac{\mathrm{ch}\lambda}{\mathrm{sh}\lambda}+\frac{q(H)H^4}{\lambda^4\mathrm{ch}\lambda}\left(\frac{1}{\Sigma EI}-\frac{1}{(E_tI_t)_{eq}+(E_bI_b)_{eq}}\right)\\
&A_2=-\lambda A_3\\
&A_4=-A_3\mathrm{sh}\lambda-\frac{q(H)H^4}{\lambda^4\mathrm{ch}\lambda}\left(\frac{1}{\Sigma EI}-\frac{1}{(E_tI_t)_{eq}+(E_bI_b)_{eq}}\right)
\end{aligned}\right\} \tag{26}$$

Substituting Eqs. (25) and (26) into Eq. (23), we can get

$$y=A_3\left(\frac{\mathrm{sh}\lambda}{\mathrm{ch}\lambda}-\lambda\xi+\mathrm{sh}\lambda\xi-\frac{\mathrm{sh}\lambda}{\mathrm{ch}\lambda}\mathrm{ch}\lambda\xi\right)+\frac{q(H)H^4}{120\Sigma EI}\xi^5+\frac{q(H)H^4}{6\Sigma EI}\xi^2+\frac{q(H)H^4}{\lambda^4\mathrm{ch}\lambda}\left(\frac{1}{\Sigma EI}-\frac{1}{(E_tI_t)_{eq}+(E_bI_b)_{eq}}\right)(1-\mathrm{ch}\lambda\xi)+\left[\frac{q(H)H^4}{6\lambda^2}\left(\frac{1}{\Sigma EI}-\frac{1}{(E_tI_t)_{eq}+(E_bI_b)_{eq}}\right)-\frac{q(H)H^4}{12\Sigma EI}\right]\xi^3 \tag{27}$$

While substituting Eqs. (14) and (21) into Eq. (10) leads to

$$M_f(z)=-\frac{q(H)H^4}{6}(2-3\xi+\xi^3)+\frac{(E_tI_r)_{eq}+(E_bI_b)_{eq}}{H^2}\frac{d^2y}{d\xi^2} \tag{28}$$

Substituting Eq. (28) into Eq. (14), the derivation of $y_{f,M}$ is

$$\frac{dy_{f,M}}{d\xi}=\frac{q(H)H^2}{6}(2-3\xi+\xi^3)-\frac{(E_tI_t)_{eq}+(E_bI_b)_{eq}}{E_fI_f}\left[\begin{aligned}&A_3\lambda\left(\mathrm{ch}\lambda\xi-\frac{\mathrm{sh}\lambda}{\mathrm{ch}\lambda}\mathrm{sh}\lambda\xi\right)+\frac{q(H)H^4}{3\Sigma EI}\xi+\frac{q(H)H^4}{24\Sigma EI}\xi^4\\&-\frac{q(H)H^4}{\lambda^3\mathrm{ch}\lambda}\left(\frac{1}{\Sigma EI}-\frac{1}{(E_tI_t)_{eq}+(E_bI_b)_{eq}}\right)\mathrm{sh}\lambda\xi\\&+\left[\frac{q(H)H^4}{2\lambda^2}\left(\frac{1}{\Sigma EI}-\frac{1}{(E_tI_t)_{eq}+(E_bI_b)_{eq}}\right)-\frac{q(H)H^4}{4\Sigma EI}\right]\xi^2\end{aligned}\right]+A_5 \tag{29}$$

From the boundary condition $y_f(0)=0$, we can get

$$A_5=\frac{(E_tI_t)_{eq}+(E_bI_b)_{eq}}{E_fI_f}A_3\lambda \tag{30}$$

Substituting Eq. (30) into Eq. (29) leads to

$$\left.\frac{dy_{f,M}}{d\xi}\right|_{\xi=1}=\frac{q(H)H^4}{8E_fI_f}-\frac{(E_tI_t)_{eq}+(E_bI_b)_{eq}}{E_fI_f}\left(\frac{1}{\Sigma EI}-\frac{1}{(E_tI_t)_{eq}+(E_bI_b)_{eq}}\right)\frac{q(H)H^4}{\lambda^2}\left(\frac{1}{2}-\frac{\mathrm{sh}\lambda}{\lambda\mathrm{ch}\lambda}\right)+\frac{(E_tI_t)_{eq}+(E_bI_b)_{eq}}{E_fI_f}A_3\lambda\left(1-\mathrm{ch}\lambda-\frac{\mathrm{sh}\lambda}{\mathrm{ch}\lambda}\mathrm{sh}\lambda\right)-\frac{(E_tI_t)_{eq}+(E_bI_b)_{eq}}{E_fI_f}\frac{q(H)H^4}{8\Sigma EI} \tag{31}$$

The shear force at the top of the frame is 0, which leads to

$$Q_f|_{\xi=1}=-(Q_t+Q_b)|_{\xi=1}=\frac{(E_tI_t)_{eq}+(E_bI_b)_{eq}}{H^3}\left.\frac{d^3y}{d\xi^3}\right|_{\xi=1}=0 \tag{32}$$

Substituting Eqs. (27) and (32) into Eq. (16), we can get

$$\left.\frac{dy_{f,Q}}{d\xi}\right|_{\xi=1}=\frac{q(H)H^4}{\lambda^3}\left(\frac{1}{\Sigma EI}-\frac{1}{(E_tI_t)_{eq}+(E_bI_b)_{eq}}\right)\frac{\Sigma EI}{E_fI_f}\left(\frac{1}{\lambda}-\frac{\mathrm{sh}\lambda}{\mathrm{ch}\lambda}\right)$$

$$+A_3\frac{\Sigma EI}{E_fI_f}\lambda\left(\mathrm{ch}\lambda-\frac{\mathrm{sh}\lambda}{\mathrm{ch}\lambda}\right) \tag{33}$$

From Eq. (27) , the derivation of y is

$$\left.\frac{dy}{d\xi}\right|_{\xi=1}=A_3\lambda\left(-1+\mathrm{ch}\lambda\xi-\frac{\mathrm{sh}\lambda}{\mathrm{ch}\lambda}\mathrm{sh}\lambda\right) \tag{34}$$

$$-\frac{q(H)H^4}{\lambda^3}\left(\frac{1}{\Sigma EI}-\frac{1}{(E_tI_t)_{eq}+(E_bI_b)_{eq}}\right)\frac{\mathrm{sh}\lambda}{\mathrm{ch}\lambda}$$

$$+\frac{q(H)H^4}{2\lambda^2}\left(\frac{1}{\Sigma EI}-\frac{1}{(E_tI_t)_{eq}+(E_bI_b)_{eq}}\right)+\frac{q(H)H^4}{8\Sigma EI}$$

The lateral displacement of the frame is composed of bending and shear lateral displacement, namely

$$\left.\frac{dy_f}{d\xi}\right|_{\xi=1}=\left.\frac{dy_{f,M}}{d\xi}\right|_{\xi=1}+\left.\frac{dy_{f,Q}}{d\xi}\right|_{\xi=1} \tag{35}$$

Substituting Eqs. (31), (33) and (34) into Eq. (35) leads to

$$A_3=\frac{q(H)H^4}{\lambda^3}\left(\frac{1}{\Sigma EI}-\frac{1}{(E_tI_t)_{eq}+(E_bI_b)_{eq}}\right)\left(\frac{1}{2}-\frac{1}{\lambda^2}\right) \tag{36}$$

Then substituting Eq. (36) into Eq. (26), we can get

$$\left.\begin{aligned}
A_1&=\frac{\mathrm{sh}\lambda}{\mathrm{ch}\lambda}\left\{\frac{q(H)H^4}{\lambda^3}\left(\frac{1}{\Sigma EI}-\frac{1}{(E_tI_t)_{eq}+(E_bI_b)_{eq}}\right)\left(\frac{1}{2}-\frac{1}{\lambda^2}\right)\right\}\\
&\quad+\frac{q(H)H^4}{\lambda^4\mathrm{ch}\lambda}\left(\frac{1}{\Sigma EI}-\frac{1}{(E_tI_t)_{eq}+(E_bI_b)_{eq}}\right)\\
A_2&=-\left\{\frac{q(H)H^4}{\lambda^2}\left(\frac{1}{\Sigma EI}-\frac{1}{(E_tI_t)_{eq}+(E_bI_b)_{eq}}\right)\left(\frac{1}{2}-\frac{1}{\lambda^2}\right)\right\}\\
A_4&=-\frac{\mathrm{sh}\lambda}{\mathrm{ch}\lambda}\left\{\frac{q(H)H^4}{\lambda^3}\left(\frac{1}{\Sigma EI}-\frac{1}{(E_tI_t)_{eq}+(E_bI_b)_{eq}}\right)\left(\frac{1}{2}-\frac{1}{\lambda^2}\right)\right\}\\
&\quad-\frac{q(H)H^4}{\lambda^4\mathrm{ch}\lambda}\left(\frac{1}{\Sigma EI}-\frac{1}{(E_tI_t)_{eq}+(E_bI_b)_{eq}}\right)
\end{aligned}\right\} \tag{37}$$

5.2. Under uniformly distributed load

Using the same solution progress as that under the inverted triangle load, we can obtain the lateral displacement under uniformly distributed load as

$$y=A_1+A_2\xi+A_3\mathrm{sh}\lambda\xi+A_4\mathrm{ch}\lambda\xi+\frac{q(H)H^4}{24\Sigma EI}(1-\xi)^4 \tag{38}$$

$$+\frac{q(H)H^4}{2\lambda^2}\left(\frac{1}{\Sigma EI}-\frac{1}{(E_tI_t)_{eq}+(E_bI_b)_{eq}}\right)\xi^2$$

where

$$A_1=-\frac{q(H)H^4}{24\Sigma EI}+\frac{q(H)H^4}{\lambda^2}\left(\frac{1}{\Sigma EI}-\frac{1}{(E_tI_t)_{eq}+(E_bI_b)_{eq}}\right)\frac{1}{\lambda\mathrm{ch}\lambda}\left\{\mathrm{sh}\lambda+\frac{1}{\lambda}\right\}$$

$$A_2=\frac{q(H)H^4}{6\Sigma EI}-\frac{q(H)H^4}{\lambda^2}\left(\frac{1}{\Sigma EI}-\frac{1}{(E_tI_t)_{eq}+(E_bI_b)_{eq}}\right)$$

$$A_3=\frac{q(H)H^4}{\lambda^3}\left(\frac{1}{\Sigma EI}-\frac{1}{(E_tI_t)_{eq}+(E_bI_b)_{eq}}\right)$$

$$A_4=\frac{q(H)H^4}{\lambda^2}\left(\frac{1}{\Sigma EI}-\frac{1}{(E_tI_t)_{eq}+(E_bI_b)_{eq}}\right)\frac{1}{\lambda\mathrm{ch}\lambda}\left\{\mathrm{sh}\lambda+\frac{1}{\lambda}\right\}$$

5.3. Under top concentrated load

Using the same solution progress as that under the inverted triangle load, we can obtain the lateral displacement under top concentrated load as

$$y=A_1+A_2\xi+A_3\mathrm{sh}\lambda\xi+A_4\mathrm{ch}\lambda\xi+\frac{PH^3}{6\Sigma EI}(1-\xi)^3 \tag{39}$$

where

$$A_1=-\frac{PH^3}{\lambda^3}\frac{E_fI_f}{\Sigma EI[(E_tI_t)_{eq}+(E_bI_b)_{eq}]}\frac{\mathrm{sh}\lambda}{\mathrm{ch}\lambda}-\frac{PH^3}{6\Sigma EI}$$

$$A_2=-\frac{PH^3}{\lambda^2}\frac{E_fI_f}{\Sigma EI[(E_tI_t)_{eq}+(E_bI_b)_{eq}]}+\frac{PH^3}{2\Sigma EI}$$

$$A_3=-\frac{PH^3}{\lambda^3}\frac{E_fI_f}{\Sigma EI[(E_tI_t)_{eq}+(E_bI_b)_{eq}]}$$

$$A_4=\frac{PH^3}{\lambda^3}\frac{E_fI_f}{\Sigma EI[(E_tI_t)_{eq}+(E_bI_b)_{eq}]}\frac{\mathrm{sh}\lambda}{\mathrm{ch}\lambda}$$

6. Simplified Calculation Formulas for Internal Forces

From Eqs. (11) and (14), it is known that the moment and shear of the hinged frame with BRBs at height ξ can be expressed as

$$\left.\begin{aligned}
M_b(\xi)&=-\frac{(E_bI_b)_{eq}}{H^2}\frac{d^2y}{d\xi^2}\\
Q_b(\xi)&=-\frac{(E_bI_b)_{eq}}{H^3}\frac{d^3y}{d\xi^3}
\end{aligned}\right\} \tag{40}$$

The moment and shear of the concrete core tube at height ξ can be expressed as:

$$\left.\begin{aligned}
M_t(\xi)&=-\frac{(E_tI_t)_{eq}}{H^2}\frac{d^2y}{d\xi^2}\\
Q_t(\xi)&=-\frac{(E_tI_t)_{eq}}{H^3}\frac{d^3y}{d\xi^3}
\end{aligned}\right\} \tag{41}$$

The moment and shear of the semi-rigid steel frame at height ξ can be expressed as:

$$\left.\begin{aligned} M_f(\xi) &= M(\xi) + \frac{(E_tI_t)_{eq} + (E_bI_b)_{eq}}{H^2}\frac{d^2y}{d\xi^2} \\ Q_f(\xi) &= Q(\xi) - \frac{(E_tI_t)_{eq} + (E_bI_b)_{eq}}{H^3}\frac{d^3y}{d\xi^3} \end{aligned}\right\} \tag{42}$$

7. Comparisons

While establishing the mechanical model, it is assumed that the horizontal links between the semi-rigid frame, BRBs and concrete core tube along the height of the building are continuous. However, in reality the links between the semi-rigid frame, BRBs and concrete tube only exist at the floor level. Therefore the assumption does not agree with the real situation. In order to identify the reasonableness of the assumption, comparisons are conducted between the results from simplified model and FEM results on an example building of the novel mixed structure.

7.1. Introduction of finite element model

The beams and columns in the frame-brace-wall model are simulated with frame element with two nodes, and each node has six degrees of freedom, as shown in Fig. 6(a). The overall concrete shear walls are simulated with layered shell element, and the layers in the shell element could simulate concrete or steel rebar by defining the thickness and material (Li, Shi, and Wang, 2009; Shihua, 2001), as shown in Fig. 6(b).

BRBs and semi-rigid connections could be simulated with two-node link element. One link element is composed of six individual "springs", and each spring corresponds to one of the six degrees of freedom (three translational and three rotational degrees of freedom). By defining the M-θ relation of a rotational spring or the N-δ relation of an axial spring, the link could simulate semi-rigid connections or BRBs respectively, as shown in Fig. 6(c) and 6(d).

7.2. Example buildings

Figure 7 shows the geometric dimension of the example buildings, and the horizontal inverted-triangle distributed load is applied on the structure. The section of the steel column is H500×500×20×24 and the section of the steel beam is H500×300×16×18 for the frame. The section of the column connected with BRB is H300×300×12×16, and the section of the beam connected with BRB is H350×200×12×14. The sections of BRBs in different models are different. The thickness of the concrete wall is 400 mm. The elastic modulus of the steel is 2.0E + 5N/mm^2; the elastic modulus of the concrete is 3.0E + 4N/mm^2; the original rotational stiffness of the semi-rigid connection for the steel frame is 1.20E + 12N*mm/rad.

7.3. Comparisons of calculation results

The overall lateral stiffness is $K=V/\Delta$, where V is the shear force at the bottom of the building, and Δ is the lateral displacement at the top of the building. Study shows that the height-width ratio of the concrete wall and the axial stiffness of the BRB have significant influence to the proportion of the shear deformation in the total deformation of the structure.

In order to illustrate the applicability and reliability of the simplified algorithm proposed, two groups of example buildings are selected, and the height -width ratios of the concrete wall are respectively $H/B = 9$ and $H/B = 3$. Seven example buildings in one group are established by modifying the stiffness of the BRBs. The results of K of the example buildings with large and small height-width ratio are listed in Table 2 and Table 3 respectively.

Comparing the relative difference of overall lateral stiffness of all the example buildings obtained between proposed formula and FEM, it is found that the largest relative difference of the stiffness is 2.13%, which demonstrates that the formulas derived in this paper are accurate enough for predicting the behavior of the new steel-concrete mixed structure.

8. Conclusions

A novel steel-concrete mixed structure is proposed in

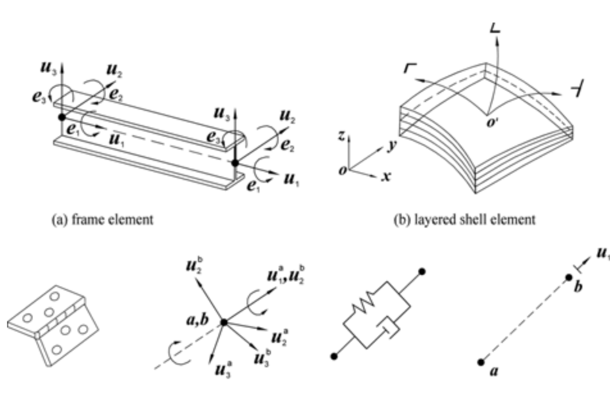

Figure 6. Elements used in the frame-brace-wall model.

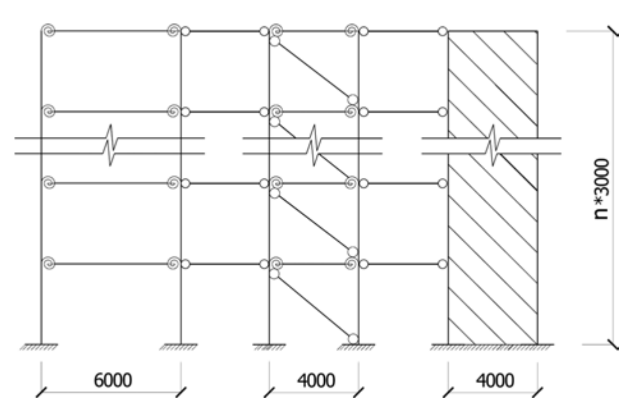

Figure 7. geometric dimension of the model.

Table 2. Results of K obtained by simplified model and FEM for examples A1~A7

Example	Axial stiffness of BRB (N/mm)	C_{bf} (N)	$1+3.64\gamma_b^2$	$(E_bI_b)_{eq}$ (N·mm^2)	K (N/mm) Theoretical formula	K (N/mm) FEM	errors%
A1	2160000	4.15E + 09	1.014	2.03E + 16	13501	13213	2.13
A2	576000	1.11E + 09	1.052	1.96E + 16	13414	13125	1.43
A3	324000	6.22E + 08	1.093	1.88E + 16	13329	13047	2.11
A4	216000	4.15E + 08	1.139	1.81E + 16	13239	12968	2.04
A5	162000	3.11E + 08	1.186	1.74E + 16	13155	12898	1.95
A6	108000	2.07E + 08	1.279	1.61E + 16	13007	12776	1.78
A7	79200	1.52E + 08	1.380	1.49E + 16	12868	12661	1.61

Table 3. Results of the K obtained by simplified model and FEM for example B1~B7

Example	Axial stiffness of BRB (N/mm)	C_{bf} (N)	$1+3.64\gamma_b^2$	$(E_bI_b)_{eq}$ (N·mm^2)	K (N/mm) Theoretical formula	K (N/mm) FEM	errors%
B1	2232000	4.29E + 09	1.121	1.84E + 16	259231	256410	1.09
B2	1260000	2.42E + 09	1.215	1.69E + 16	254762	253165	0.63
B3	900000	1.73E + 09	1.301	1.58E + 16	251224	250313	0.36
B4	576000	1.11E + 09	1.471	1.40E + 16	245468	245700	0.09
B5	432000	8.29E + 08	1.628	1.27E + 16	241207	242229	0.42
B6	324000	6.22E + 08	1.837	1.12E + 16	236658	238474	0.76
B7	223200	4.29E + 08	2.215	9.30E + 15	230619	233100	1.06

this paper to improve the seismic behavior of conventional steel-concrete mixed structures. The simplified algorithms to predict the lateral displacements and internal forces of the novel mixed structure under inverted-triangle distributed load, uniformly distributed load and top-concentrated load are derived based on structural elastic theory. The conclusions may be drawn as follows:

(1) Although the links between the semi-rigid frames, BRBs and concrete tube only exist at floor levels, it is reasonable to assume that the horizontal links along the height of the building are continuous when establishing the mechanical model.

(2) The effectiveness of the simplified algorithm is verified by FEM comparisons. The formulas proposed in this paper are accurate enough to predict the lateral displacements and internal forces of the mixed structure.

Acknowledgements

The work reported hereinabove is financially supported by the National Science Foundation of China through the project No. 90815029, which is gratefully acknowledged.

References

Anli, K. C. (2005). Dynamics of Structures: Theory and Applications to Earthquake Engineering, Second Edition. Higher Education Press, Beijing, China.

Bao, S. (2001). New high-rise building (2nd ed.). China water-power press/Intellectual property rights press, Beijing, China.

Chinese code.(1998). Technical specification for steel structure of tall buildings(JGJ99-98). Beijing: China architecture and building press.

Duane, K. M. (1998). "Lessons learned from the Northridge earthquake." Engineering Structures, 20(4-6), pp. 249~260.

Eurocode 4. (2004). Design of steel and concrete structures Part1-1: General rules and rules for building, European Committee for Standardization, Brussels.

Gregory, G. D. and Hiroshi, N. C. (2004). "Overview of U.S.-Japan Research on the seismic Design of Composite Reinforced concrete and steel Moment Frame structures." Journal of Structural Engineering, 130(2), pp. 361~367.

Hu, D. (2008). Practical seismic design method of semi-rigid composite frame: [PhD dissertation of Tongji university]. Tongji university, Shanghai, China.

Koz, L. S. (2002). "Analysis of steel and composite braced frames with semi-rigid joints" Advance in steel structures, 1, pp. 269~276.

Li, G. Q., Shi, W. and Wang, J. (2009). Design of the semi-rigid steel frame structure. China architecture and building press, Beijing, China.

Li, L. (2011). Seismic Design approach and seismic behavior study on novel multi-lateral resistant steel-concrete mixed structure: [PhD dissertation of tongji university]. Tongji university, Shanghai, China.

Lu, T., Qin, S. and Luo, Y. (2009). "Pseudo dynamic experimental study on high-rise steel-concrete hybrid structure." Journal of Building Structures, 30(3), pp. 27~35.

Wang, C. K., Tian, C. and Xiao, C. (2011). "Development of research and application of concrete-steel hybrid high-rise building strucutres." Building Structure, 41(11), pp. 28~33.

Wang, D. S. and Zhou, J. (2010). "Development and prospect of hybrid high-rise building structures in China." Journal of Building Structures, 31(6), pp. 62~70.

Yao, Z. L., Bai, G. L., and Dang, F. (2010) "Analysis on a steel-concrete hybrid structure temperature effect and supporting block design." Applied Mechanics and Materials, 29/30/31/32, pp. 1862~1865.